

Research Article

Olmesartan Improves Hepatic Sinusoidal Remodeling in Mice with Carbon Tetrachloride-Induced Liver Fibrosis

Ying Wu ¹, Xue Ge ², Si-Ning Wang ³, and Chun-Qing Zhang ³

¹Department of Gastroenterology, The Second Hospital, Cheeloo College of Medicine, Shandong University, Jinan, Shandong, China

²Department of Intensive Care Unit, The Second Hospital, Cheeloo College of Medicine, Shandong University, Jinan, Shandong, China

³Department of Gastroenterology, Shandong Provincial Hospital, Cheeloo College of Medicine, Shandong University, Jinan, Shandong, China

Correspondence should be addressed to Chun-Qing Zhang; zhangchunqing_sdu@163.com

Received 9 January 2022; Revised 4 July 2022; Accepted 30 July 2022; Published 26 August 2022

Academic Editor: Koichiro Wada

Copyright © 2022 Ying Wu et al. This is an open access article distributed under the Creative Commons Attribution License, which permits unrestricted use, distribution, and reproduction in any medium, provided the original work is properly cited.

Aim. In mice with liver fibrosis produced by carbon tetrachloride (CCl₄), the effects of olmesartan on intrahepatic angiogenesis and sinusoidal remodeling will be evaluated. **Methods.** By injecting CCl₄ into the peritoneal cavity, we established a mouse model of liver fibrosis. Using Sirius red and Masson trichrome staining, the extent of liver fibrosis in the animals was determined. Using immunohistochemical labeling and western blotting, the level of α -smooth muscle actin (α -SMA) expression, a characteristic of hepatic stellate cell activation, was assessed. Electron microscopy was used to determine the effect of olmesartan on hepatic sinusoidal capillarization, and immunohistochemical labeling was used to determine the expression levels of endothelial and basement membrane proteins in mouse liver tissues. Platelet-derived growth factor (PDGF), IL-10, vascular endothelial growth factor (VEGF), and angiotensin II levels in mouse serum were measured by Luminex multifactor analysis and ELISA. Olmesartan's effect on the angiotensin II type 1 receptor (AT1R) and the VEGF receptor (VEGFR) was evaluated using western blotting. **Results.** Olmesartan reduced CCl₄-induced inflammatory cell infiltration and collagen deposition to alleviate liver fibrosis. α -SMA expression was decreased, and HSC activation was inhibited in mouse liver tissues by olmesartan treatment. In addition, hepatic sinusoidal capillarization was improved under the action of olmesartan. The expression of collagen IV, fibronectin, CD31, and von Willebrand factor (VWF) in the olmesartan group was also markedly downregulated. In fibrotic mice, olmesartan medication decreased the levels of PDGF, VEGF, and angiotensin II, but it increased the level of IL-10. Moreover, olmesartan reduced the expression of VEGFR-1, VEGFR-2, and AT1R relative to CCl₄-induced liver fibrosis. **Conclusions.** In mice with CCl₄-induced fibrosis, olmesartan lowers angiogenesis and improves hepatic sinusoidal remodeling, according to our findings. By acting on the angiotensin II-AT1R-VEGF axis, this is achieved.

1. Introduction

Portal hypertension can lead to splenomegaly, ascites, and esophageal varices and is the prime cause of high mortality in cirrhosis patients [1]. In liver fibrosis and cirrhosis, excessive extracellular matrix (ECM) deposition, the formation of regenerative nodules, and construction and remodeling of hepatic sinusoidal vessels lead to increased sinus resistance and portal pressure [2]. Sinusoidal resistance, fibrosis, and portal hypertension are all linked to intrahepatic angiogenesis

and sinusoidal remodeling, according to study [1]. The emergence of neoangiogenesis and abnormal vascular structures in the liver are closely connected with the progression of chronic liver disease [3, 4]. Understanding the relationship between angiogenesis and fibrogenesis may give a novel treatment strategy for liver fibrosis and portal hypertension [5, 6].

The complex vascular structure known as the hepatic sinusoid is comprised of hepatic stellate cells (HSCs) whose cell processes surround the sinusoid, liver sinusoidal

endothelial cells (LSECs) that constitute the sinus wall, Disse space between LSECs and hepatocytes, and Kupffer cells. HSCs and LSECs play key roles in increasing liver vascular resistance. Activated HSCs contribute to fibrogenesis and the reconstitution of intrahepatic structures through cell proliferation and ECM production [1, 7, 8]. In addition, LSEC phenotypic modifications and increased number of contractile HSCs surrounding LSECs are hallmarks of sinusoidal vascular remodeling [9]. In liver fibrosis and cirrhosis, LSECs lose their fenestrae, totally form a continuous basement membrane, and undergo capillarization [10]. The formation of LSEC capillarization accelerates HSC activation and fibrogenesis, and the disappearance of the normal filtration barrier results in changes in liver microcirculatory functions [4]. On the other hand, activated HSCs secrete angiogenic molecules that stimulate LSECs, thereby promoting angiogenesis [1, 11]. The amelioration of liver fibrosis by particular angiogenesis-inhibiting drugs, such as those that target vascular endothelial growth factor receptor-2 (VEGFR-2), demonstrates the importance of angiogenesis in fibrogenesis [1, 12].

The renin-angiotensin system (RAS) is vital for maintaining electrolyte balance and blood pressure stability [13, 14]. The angiotensin II type 1 receptor (AT1R) is one of the RAS components that activated HSCs may express [15]. When liver fibrosis occurs, local intrahepatic angiotensin II levels increase and angiotensin II binds with AT1R on the surface of HSCs to promote HSC activation, proliferation, and contraction through multiple signal transduction pathways [16, 17]. Angiotensin II receptor blockers have been shown in animal experiments to modulate the RAS in the treatment of liver fibrosis; however, the specific molecular mechanism is still unclear [18, 19]. Angiotensin II is a potent vascular smooth muscle cell growth factor that, according to studies [20, 21], upregulates VEGF and induces angiogenesis. In addition, the AT1R antagonist candesartan has been shown to diminish angiogenesis in hepatocellular carcinoma by blocking the VEGF pathway [20]. The present study examined the effect of the AT1R antagonist olmesartan on the inhibition of angiogenesis and improvement of sinusoidal remodeling via the RAS in fibrotic mice.

2. Materials and Procedures

2.1. Animal Model Construction. MedChemExpress (NJ, USA) provided olmesartan for our experiment. Shandong University's Experimental Animal Center (Jinan, China) supplied 30 adult male C57BL/6 mice, which were housed under constant environmental temperature (23–25°C). All the animals were provided with a consistent diet and unrestricted water. The animal care and utilization committee at Shandong University approved the experimental protocols.

For this study, a mouse model of liver fibrosis was developed using our previous methods [22]. Three types of mice were randomly selected from the animal population: (1) a normal control category, in which mice received intraperitoneal injections of olive oil (5 ml/kg) twice weekly for 8 weeks, (2) the carbon tetrachloride (CCl₄) category, in which fibro-

sis was induced by intraperitoneal injections of CCl₄ in olive oil (30 percent, 5 ml/kg) twice weekly for 8 weeks, and (3) the CCl₄ + olmesartan (5 mg/kg/d) category, in which mice were administered CCl₄ (30 percent, 5 ml/kg) for the first 2 weeks and then administered both drugs for the next 6 weeks. The survival percentage for mice at the completion of the experiment was 80%.

2.2. Cytokine ELISA. The blood samples were obtained after the mice had been sedated and centrifuged for 10 minutes at 3000 rpm, and the supernatants were collected. In accordance with the manufacturer's instructions, an ELISA kit (RayBiotech, GA, US) was used to quantify the quantity of angiotensin II in each category's serum. Using a scanning MultiWell spectrophotometer, the absorbance at 450 nm was measured (BioRad Model 550, CA, US). ELISACalc software was used to plot the standard curve and calculate the angiotensin II concentrations in samples. The results were analyzed with GraphPad Prism 7.0.

2.3. Luminex Analysis. Blood samples from mice were centrifuged and collected using the method described above. The relevant biomarkers (platelet-derived growth factor (PDGF), IL-10, and VEGF) in mouse serum were measured following the instructions using a R&D LXSAMSM-09 Luminex System. The data were analyzed with GraphPad Prism 7.0.

2.4. Histopathological Examination. Paraffin slices of liver tissue were stained with masson trichrome, sirius red, and hematoxylin and eosin using conventional procedures. The METAVIR scale rated the severity of liver fibrosis (0 for no fibrosis, 1 for portal fibrosis, 2 for periportal fibrosis, 3 for bridging fibrosis, and 4 for cirrhosis) [23].

2.5. Immunohistochemistry. The liver slices were deparaffinized, serially dehydrated with ethanol, and subjected to the heat-induced antigen retrieval process. The sections were then blocked, followed by overnight primary antibody incubation at 4°C. α -Smooth muscle actin (α -SMA) (1:400, Abcam, MA, US), collagen IV (1:1000, Abcam, MA, US), fibronectin (1:2000, Abcam, MA, US), CD31 (1:2000, Abcam, MA, US), and VWF (1:200, Proteintech, IL, US) were the primary antibodies used in this study. The sections were stained with diaminobenzidine and hematoxylin after being subjected to the biotinylated secondary antibody. Under a light microscope, the positively stained areas appeared brownish-yellow. The results were analyzed with Image-Pro Plus 6.0.

2.6. Transmission and Scanning Electron Microscopy (TEM and SEM). Fresh mouse liver tissue slices were fixed in special fixation solution for two hours and then postfixed in 1 percent osmic acid buffer solution for two hours. After ethanol dehydration, the samples were infiltrated, embedded, and aggregated. Following this, the resin blocks were chopped into thin sections and coloured with an alcohol solution containing 2% uranium acetate. TEM (HT7800/HT7700, Hitachi, Tokyo, Japan) was used to inspect and photograph the materials.

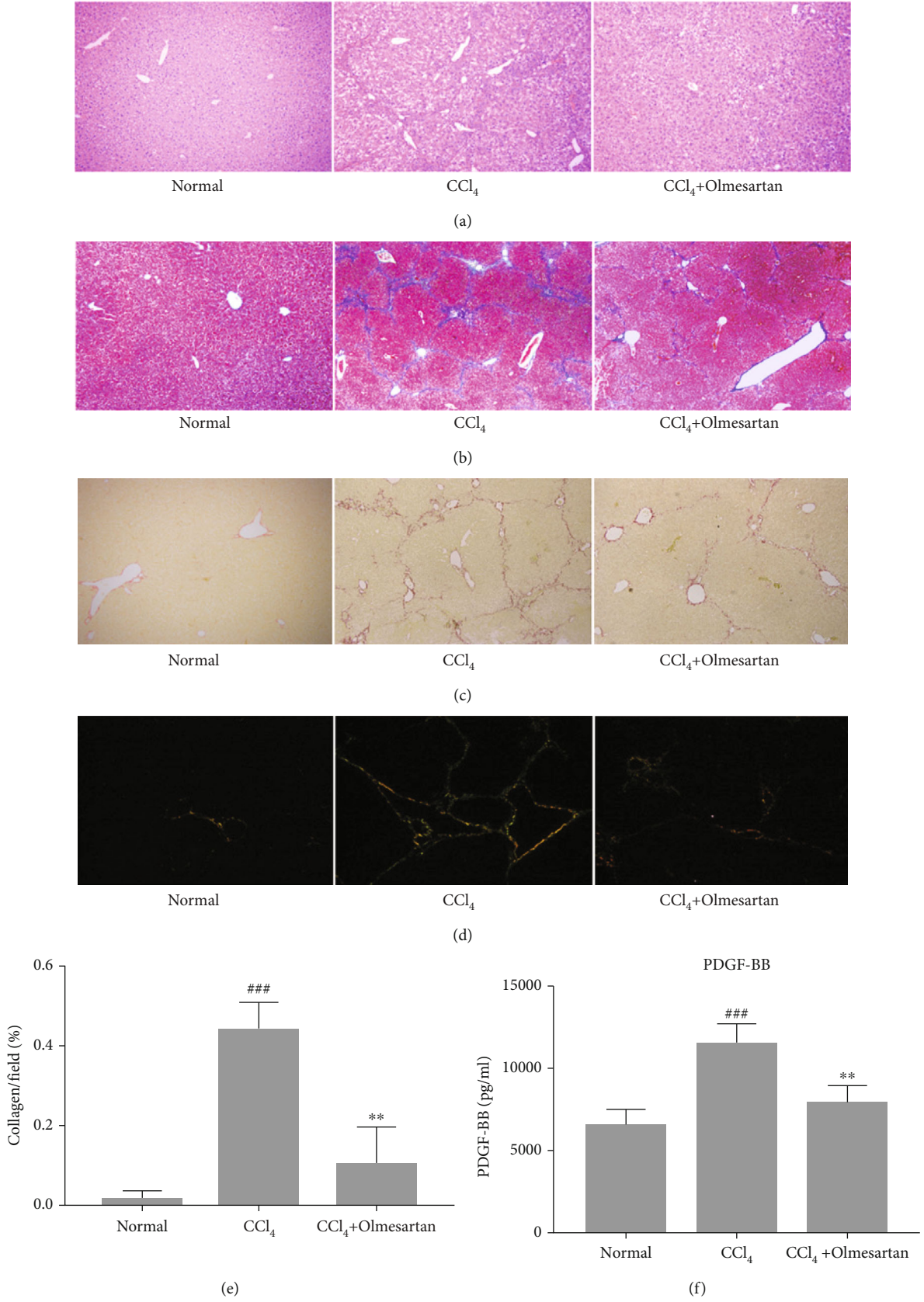


FIGURE 1: Continued.

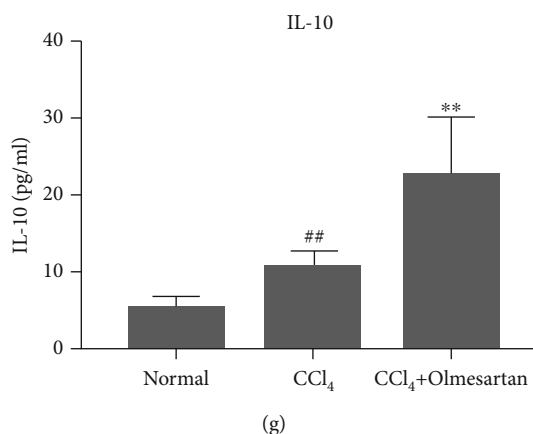
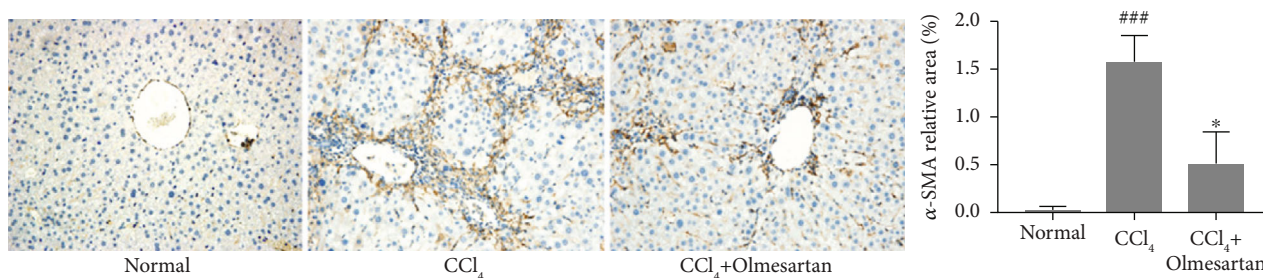
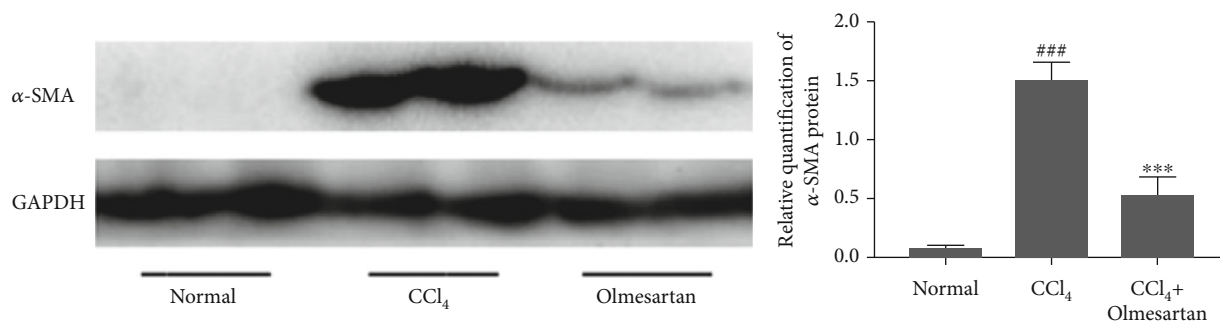


FIGURE 1: Effects of olmesartan on hepatic fibrosis and collagen production in mice treated with CCl₄. (a, b) H&E and Masson trichrome dyeing of liver tissues in different groups of mice were photographed. (c-e) The sirius red staining (polarized light shown in (d)) of liver tissues in different groups was observed, and the quantity of collagen production in each group was determined. Magnification $\times 100$. (f, g) Serum PDGF-BB and IL-10 levels were measured. ### $P < 0.001$ versus normal; ## $P < 0.01$ versus normal; ** $P < 0.01$ versus CCl₄.



(a)



(b)

FIGURE 2: Effects of olmesartan on HSC activation in CCl₄-induced fibrotic mice. (a) α -SMA immunohistochemistry was performed on mouse liver tissues from each group (magnification $\times 200$). (b) The levels of α -SMA expression in mouse liver tissues were determined by western blot. ### $P < 0.001$ versus normal; *** $P < 0.001$ versus CCl₄; * $P < 0.05$ versus CCl₄.

For scanning electron microscopy, fixed tissues were serially dehydrated in ethanol and dried in a Quorum K850 critical point drier. Following conductive treatment in an IXRF MSP-2S ion sputtering analyzer, the images were captured with a Hitachi SU8010 scanning electron microscope.

2.7. Western Blot Analysis. To conduct a western blot study on liver tissue proteins, the protein concentration of each sample was determined using a BCA protein quantification kit. The protein samples were electrophoresed on 8–12 per-

cent SDS-PAGE gels prior to being transferred to polyvinylidene fluoride filter membranes. The membranes with protein were first treated for the duration of a night at 4°C with primary antibodies before being blocked for one hour. After incubation with secondary antibodies and washing with TBST buffer, the protein bands were examined using a Millipore-enhanced chemiluminescence test kit. Using ImageJ, the optical densities of the bands were analyzed.

2.8. Statistical Analysis. Mean and standard deviation are used to illustrate the data. For the statistical analysis, the

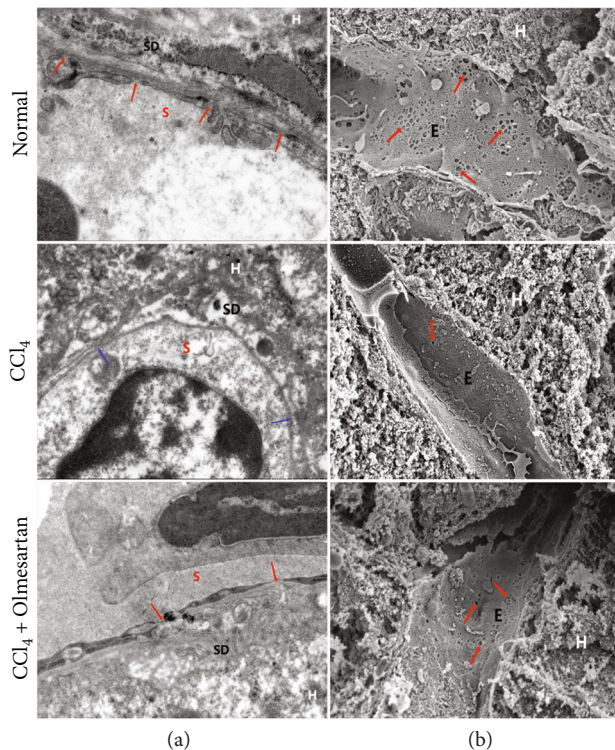


FIGURE 3: (a) A transmission electron micrograph depicting hepatic sinusoids in mice liver tissues. Representative images showed changes in the endothelial fenestrae and capillarization of the sinusoid in fibrotic mice. The fenestration structure of the mice in the CCl_4 group disappeared, and a continuous basement membrane was formed (as indicated by blue arrows), while multiple fenestrae were seen in the hepatic sinusoids of the normal mice and the olmesartan-treated mice (as shown by red arrows). S is the sinusoid, SD is the Disse space, and H is the hepatocyte. (b) A scanning electron micrograph of fenestrae in the sinusoidal endothelium of the liver of mice (as indicated by red arrows). There is defenestration of the endothelium in the CCl_4 group. E is the endothelial cell, and H is the hepatocyte. Magnification $\times 10\text{ k}$.

one-way ANOVA or Student's *t*-test was used. For all tests, values of $P < 0.05$ were considered statistically significant.

3. Results

3.1. Effects of Olmesartan on Hepatic Fibrogenesis and Injury. Olmesartan's effect on CCl_4 -induced hepatic fibrosis was determined using pathological staining (Figures 1(a)–1(d)). In the CCl_4 group, the liver architecture was much more disordered than that in the normal group and hepatic sinusoids could no longer be identified. After 8 weeks of CCl_4 injections, liver tissues exhibited increased inflammation and fibrous connective tissues (Figure 1(a)) (METAVIR more than 2). Masson trichrome and Sirius red staining revealed visible collagen production and the establishment of fibrous septa across the portal regions in the CCl_4 group. However, olmesartan alleviated these changes (Figures 1(b) and 1(c)) (METAVIR no more than 2). Under polarized light, Sirius red staining revealed that mice administered just CCl_4 had much more collagens I and III (shown in red and green,

respectively) deposited in their livers. In contrast, olmesartan medication decreased collagen production in the periportal zones, interlobular septum, and perisinusoidal spaces (Figures 1(c)–1(e)).

PDGF signaling is crucial during HSC activation and angiogenesis. The results demonstrated that olmesartan decreased the expression of PDGF-BB, although serum PDGF-BB levels were higher in CCl_4 -injected fibrotic mice than in normal mice (Figure 1(f)). IL-10 is a potential anti-inflammatory factor that can inhibit the expression of a variety of proinflammatory mediators. According to the results, IL-10 expression levels in the olmesartan group were notably higher than those in the CCl_4 group (Figure 1(g)).

3.2. Effects of Olmesartan on HSC Activation. After HSC activation, the expression of α -SMA, a critical marker associated with liver fibrosis, is increased. According to immunohistochemical labeling, α -SMA-positive cells were located along the endothelia of hepatic sinusoids in the CCl_4 -administered mice. The sinusoidal walls of unaffected mice lacked any visible positive staining. Olmesartan therapy produced significantly less α -SMA-positive cells than the CCl_4 group (Figure 2(a)). In addition, western blot test findings revealed that olmesartan medication lowered the protein expression of α -SMA (Figure 2(b)).

3.3. Effects of Olmesartan on the Hepatic Sinusoidal Capillarization of Mice. Fenestrae are round or pore-like features that penetrate the cytoplasm of sinusoidal endothelial cells, as described in reference [24]. According to TEM and SEM detections of mouse hepatic sinusoids, the LSECs of the normal control group contained plenty of fenestrae with a discontinuous basement membrane. In mice administered CCl_4 , the fenestrae of the hepatic sinusoids shrank or disappeared and the basal side of LSECs established a continuous basement membrane. However, mice treated with olmesartan showed more fenestrae than those treated with CCl_4 alone (Figure 3).

Collagen IV and fibronectin, the two major proteins that compose the basement membrane, are seldom expressed in healthy liver tissues. Immunohistochemical labeling revealed that these two proteins were remarkably elevated in the group with CCl_4 -induced hepatofibrosis and diminished in the group treated with olmesartan (Figures 4(a) and 4(b)).

3.4. Olmesartan's Effects on Intrahepatic Angiogenesis in Fibrotic Mice through the $\text{AT1R}/\text{VEGF}$ Pathway. Inhibition of intrahepatic angiogenesis has become a new target of drug therapy for liver fibrosis and portal hypertension. CD31 and VWF, which are common vascular endothelial markers, are seldom seen in the hepatic sinusoids of a healthy liver. Immunohistochemical staining indicated that CD31 and VWF expression was much higher in the CCl_4 group than that in other groups. However, the expression of these two proteins was reduced after olmesartan treatment, indicating that olmesartan inhibited CCl_4 -induced intrahepatic angiogenesis (Figures 5(a) and 5(b)).

VEGF significantly facilitates endothelial cell proliferation and intrahepatic angiogenesis. VEGFR-1 and VEGFR-

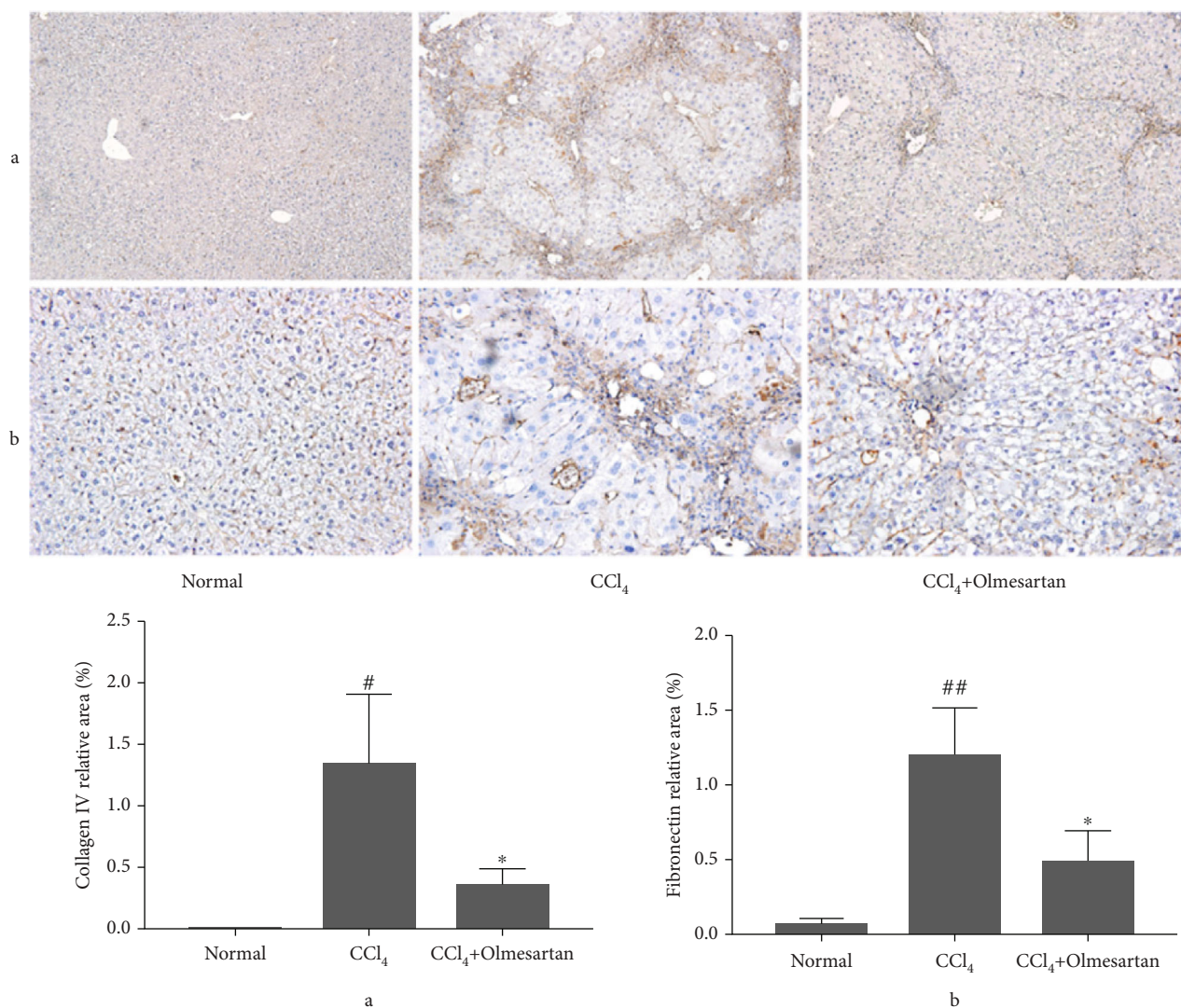


FIGURE 4: The effects of olmesartan on the proteins that compose the liver's basement membrane in fibrotic mice. (a, b) Immunohistochemistry found collagen IV and fibronectin in the liver tissues of mice from each group (magnification $\times 200$). ^{##} $P < 0.01$ vs normal; [#] $P < 0.05$ versus normal; ^{*} $P < 0.05$ vs CCl₄.

2 are two tyrosine kinase receptors with high affinity that are principally responsible for VEGF activity. The western blot results indicated that VEGFR-1 and VEGFR-2 protein expression in CCl₄-induced fibrotic livers was notably increased, while the protein expression levels of these two receptors in the olmesartan treatment group were downregulated (Figures 5(c)-5(e)).

We examined the levels of angiotensin II, AT1R, and VEGF in mice treated with olmesartan. Blood levels of angiotensin II were considerably higher in the CCl₄-induced fibrosis group compared with the normal group, but clearly lower in the olmesartan group (Figure 6(a)). In addition, we found that CCl₄ increased hepatic AT1R expression, but olmesartan downregulated angiotensin II-induced AT1R protein expression (Figure 6(b)). In the CCl₄-induced liver fibrosis group, angiotensin II promoted the production of VEGF, while olmesartan dramatically reduced angiotensin II-induced VEGF production (Figure 6(c)).

4. Discussion

Hepatic fibrosis is a pathological condition characterized by excessive ECM production and inflammatory cell infiltration [25]. Cirrhosis, portal hypertension, and even liver cancer may occur from hepatic fibrosis. Sinusoidal capillarization and hepatic angiogenesis have the greatest impact on the development of liver fibrosis and cirrhosis [26]. ARBs have been shown to lessen the severity of liver fibrosis in rats, but the molecular mechanism behind this benefit is not very clear [18, 27]. As a long-lasting ARB, olmesartan has been indicated to be more effective than other ARBs in lowering blood pressure [28, 29]. In our study, the effects of olmesartan on hepatic sinusoidal capillarization and angiogenesis in the liver fibrosis model mice were investigated.

By injecting intraperitoneal CCl₄ for eight weeks, we were able to successfully generate a mouse model of liver fibrosis. According to pathological staining, olmesartan

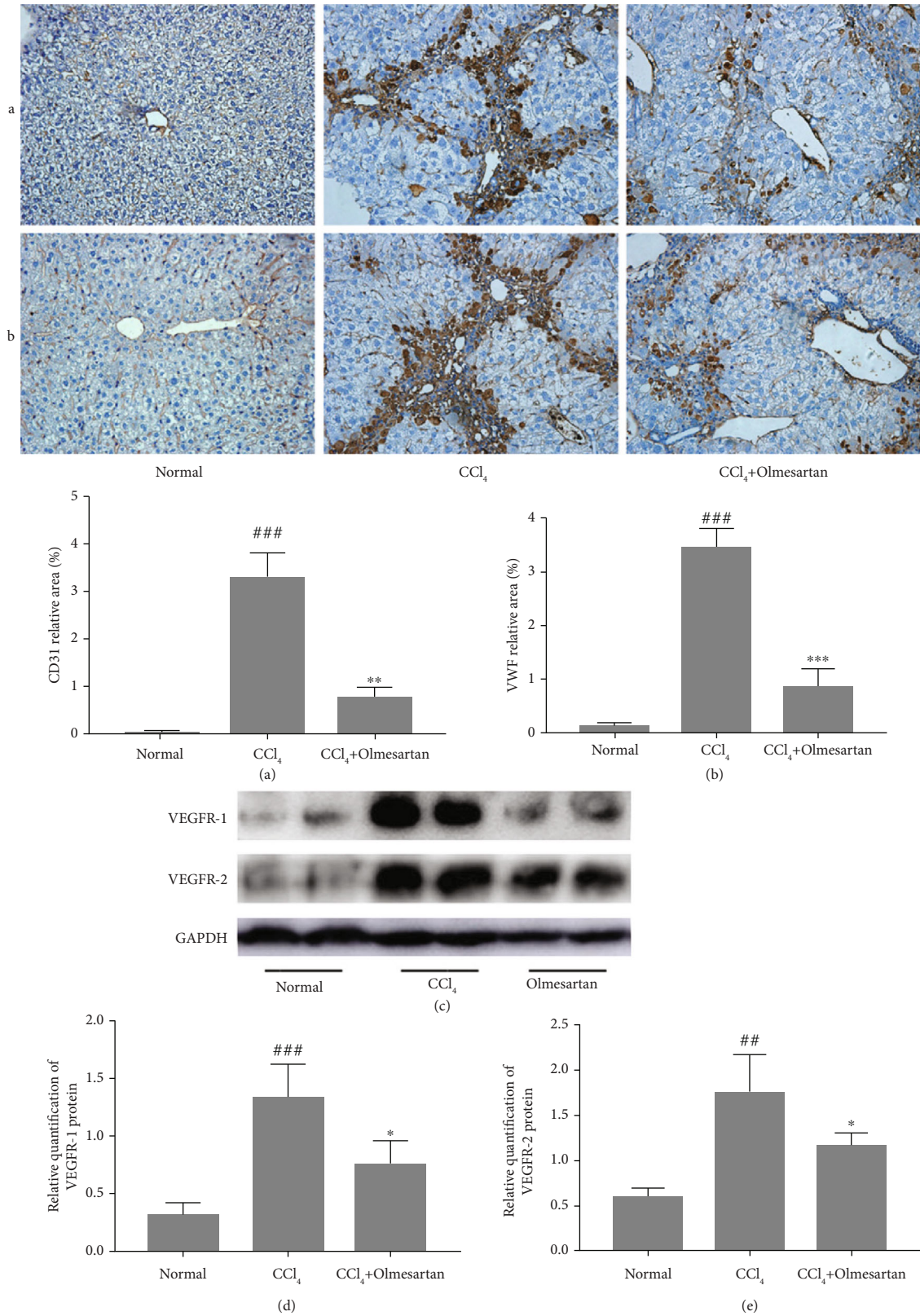


FIGURE 5: The impact of olmesartan on intrahepatic angiogenesis in mice with fibrotic livers. (a, b) Immunohistochemical staining of CD31 and VWF in liver tissues of mice (magnification $\times 200$). (c-e) Utilizing a western blot technique, the expression levels of VEGFR-1 and VEGFR-2 in liver tissues were determined. ### $P < 0.001$ versus normal; ## $P < 0.01$ versus normal; *** $P < 0.001$ versus CCl₄; ** $P < 0.01$ versus CCl₄; * $P < 0.05$ versus CCl₄.

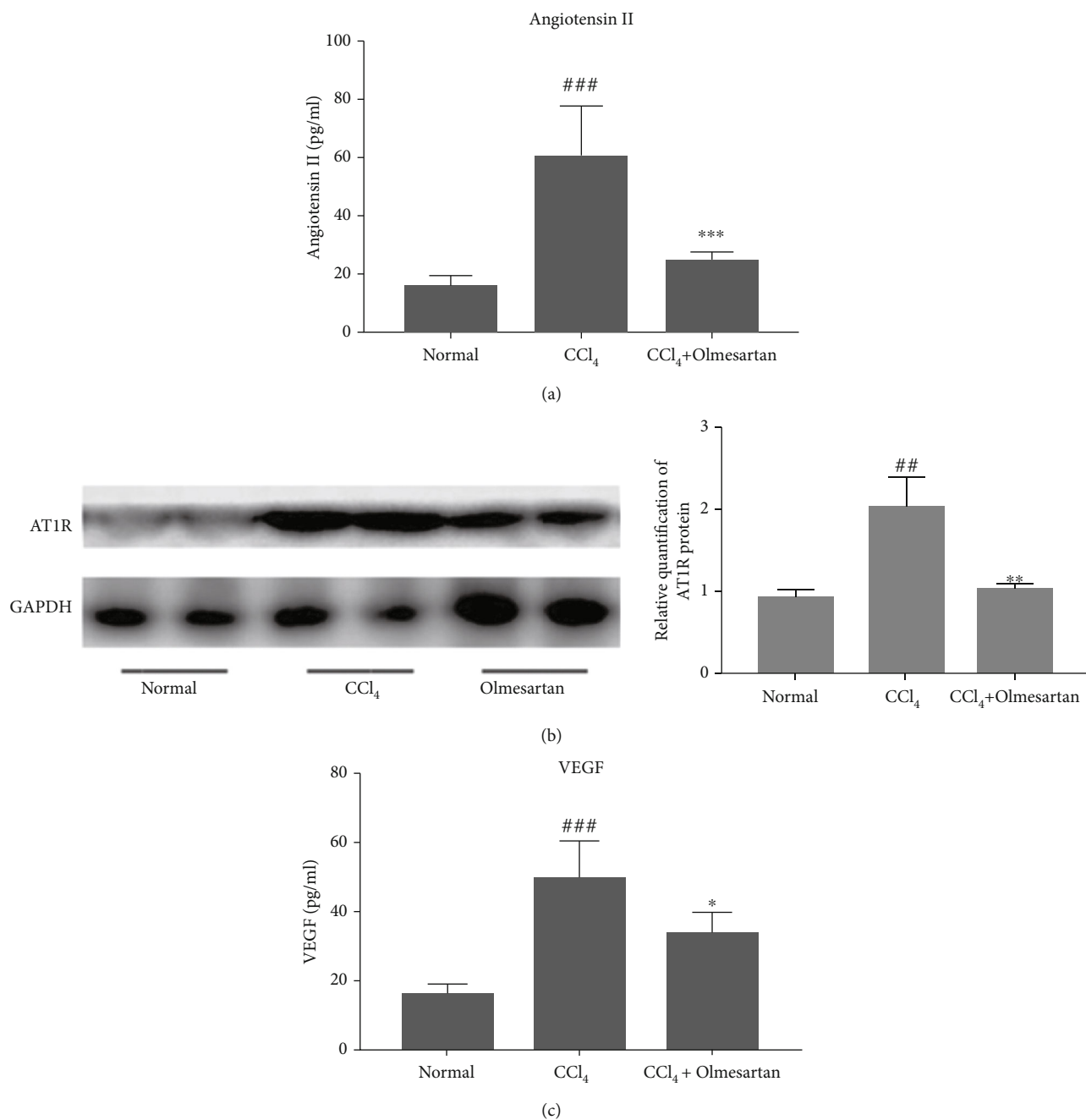


FIGURE 6: The impact of olmesartan on the AT1R/VEGF pathway in mice with hepatic fibrosis. (a) Serum levels of angiotensin II were measured. ^{###} $P < 0.001$ versus normal; ^{***} $P < 0.001$ versus CCl₄. (b) Western blot analysis was used to determine the AT1R expression levels in liver tissues. ^{##} $P < 0.01$ versus normal; ^{**} $P < 0.01$ versus CCl₄. (c) Serum levels of VEGF were measured. ^{###} $P < 0.001$ versus normal; ^{*} $P < 0.05$ versus CCl₄.

significantly lowered collagen deposition, inflammation, and fibrosis in mouse liver tissues compared to those in the CCl₄ group. HSCs have been confirmed to make a crucial impact in the progression of hepatic fibrosis [30]. In addition, α -SMA is a common marker for assessing HSC activity and proliferation [31]. When HSCs are activated with CCl₄, α -SMA expression and ECM component deposition increase. Western blot and immunohistochemical staining revealed that olmesartan inhibited α -SMA expression and the activation of HSCs. PDGF-BB may enhance the collagen I and α -

SMA levels, according to our previous studies [5]. PDGF is the most potent proliferation-stimulating factor of HSCs and can promote HSC activation, motility, and migration after binding to its receptor [32]. Therefore, blocking PDGF signaling can alleviate liver fibrosis and angiogenesis [33]. In the present study, the serum PDGF levels in mice in the liver fibrosis group were markedly increased, but olmesartan reduced PDGF expression to attenuate intrahepatic angiogenesis and fibrosis. In addition to regulating inflammatory mediators, IL-10 can promote HSC apoptosis and affect

ECM remodeling, thereby inhibiting fibrosis [34–36]. We demonstrated that CCl_4 treatment lowered serum IL-10 levels in mice, while olmesartan increased IL-10 expression, indicating that olmesartan has potential anti-inflammatory and antifibrotic effects.

Normal LSECs have characteristic fenestrae that are organized into groups of sieve plates, which can maintain liver microcirculation and homeostasis [37]. In chronic liver diseases, LSECs lose the unique fenestrated phenotype and their normal functions; this process is known as capillarization [38]. LSEC capillarization promotes HSC activation and angiogenesis in the progression of hepatic fibrosis [39–41]. In the early stages of liver fibrosis, the crosstalk between LSECs and HSCs promotes angiogenesis and fibrogenesis [33]. In addition, excessive ECM deposition and LSEC capillarization can change liver architecture and increase sinusoidal resistance, ultimately leading to portal hypertension [42]. In our present study, the TEM and SEM results demonstrated that LSEC fenestrae in the CCl_4 treatment group were decreased in number or disappeared and the basement membrane was formed, which led to capillarization and sinusoid remodeling. In addition, collagen IV and fibronectin, which are basement membrane proteins, were prominently increased in the livers of fibrotic mice, but olmesartan treatment reduced the expression of these proteins and attenuated hepatic sinusoidal capillarization. Moreover, we evaluated the effect of olmesartan on the expression of endothelial cell markers VWF and CD31. Compared with the CCl_4 -treated group, olmesartan downregulated CD31 and VWF protein expression. These findings demonstrate that olmesartan inhibits hepatic angiogenesis and alleviates hepatic sinus pressure and sinusoidal remodeling, which may improve hepatic fibrosis and portal hypertension.

Angiogenesis, the hypoxia-induced formation of new blood vessels from existing ones, is a pivotal stage in the progression of chronic liver disease [43]. VEGF, which is derived from hepatocytes and HSCs, is the most important regulator of angiogenesis and can act on LSECs and HSCs in an autocrine and paracrine manner [44]. VEGF may stimulate endothelial cell proliferation, promote the creation of endothelium tubules, and substantially contribute to the early phases of neovascularization, according to studies [45]. Additionally, LSECs exhibit an increase in VEGFR-1 and VEGFR-2 receptor expression in response to VEGF production [45]. In this study, the expression of VEGF and VEGF receptors was greatly increased in the CCl_4 -induced fibrotic group, while olmesartan decreased both. These results indicate that olmesartan can ameliorate intrahepatic angiogenesis, sinusoidal remodeling, and capillarization by inhibiting VEGF signaling.

As previously established, angiotensin II may promote HSC activation, proliferation, and contraction in vitro. In turn, active HSCs may express RAS components such as AT1R and produce angiotensin II [17]. Studies have reported that angiotensin II may upregulate VEGF to stimulate angiogenesis and that its cellular effects are mediated mainly by AT1R [20, 21]. We investigated the effects of olmesartan on protein levels of VEGF and AT1R in mice

with liver fibrosis. AT1R expression was shown to be favorably associated with VEGF expression. Our findings suggested that angiotensin II facilitated HSC activation and upregulated AT1R protein expression, thereby increasing VEGF secretion in HSCs, and that effect was reversed by olmesartan. Therefore, these findings demonstrate that olmesartan, an AT1R antagonist, inhibits angiogenesis in mice with liver fibrosis through the angiotensin II-AT1R-VEGF axis.

5. Conclusion

Our findings demonstrate that the AT1R antagonist olmesartan suppresses HSC activation and collagen deposition in liver fibrotic mice and has the effect of anti-angiogenesis and improving hepatic sinusoidal remodeling through the angiotensin II-AT1R-VEGF axis. Olmesartan may be an effective treatment agent for hepatic fibrosis and portal hypertension targeting neovascularization.

Data Availability

Upon request, the corresponding author may give the data used to support the study's results.

Conflicts of Interest

According to the authors, there are no conflicts of interest associated with the publication of this work.

Acknowledgments

This research was supported by Shandong Provincial Natural Science Foundation (no. ZR2021MH389).

References

- [1] D. Thabut and V. Shah, "Intrahepatic angiogenesis and sinusoidal remodeling in chronic liver disease: new targets for the treatment of portal hypertension?," *Journal of Hepatology*, vol. 53, no. 5, pp. 976–980, 2010.
- [2] J. García-Pagán, J. Gracia-Sancho, and J. Bosch, "Functional aspects on the pathophysiology of portal hypertension in cirrhosis," *Journal of Hepatology*, vol. 57, no. 2, pp. 458–461, 2012.
- [3] K. Brusilovskaya, P. Königshofer, P. Schwabl, and T. Reiberger, "Vascular targets for the treatment of portal hypertension," *Seminars in Liver Disease*, vol. 39, no. 4, pp. 483–501, 2019.
- [4] Q. Yao, Y. Lin, X. Li, X. Shen, J. Wang, and C. Tu, "Curcumin ameliorates intrahepatic angiogenesis and capillarization of the sinusoids in carbon tetrachloride-induced rat liver fibrosis," *Toxicology Letters*, vol. 222, no. 1, pp. 72–82, 2013.
- [5] Z. Li, Q. Ding, L. P. Ling et al., "Metformin attenuates motility, contraction, and fibrogenic response of hepatic stellate cells in vivo and in vitro by activating AMP-activated protein kinase," *World Journal of Gastroenterology*, vol. 24, no. 7, pp. 819–832, 2018.
- [6] L. J. Kong, H. Li, Y. J. Du et al., "Vatalanib, a tyrosine kinase inhibitor, decreases hepatic fibrosis and sinusoidal

- capillarization in CCl₄-induced fibrotic mice,” *Molecular Medicine Reports*, vol. 15, no. 5, pp. 2604–2610, 2017.
- [7] T. Kisseleva, “The origin of fibrogenic myofibroblasts in fibrotic liver,” *Hepatology (Baltimore, Md)*, vol. 65, no. 3, pp. 1039–1043, 2017.
- [8] P. N. Mimche, C. M. Lee, S. M. Mimche et al., “EphB2 receptor tyrosine kinase promotes hepatic fibrogenesis in mice via activation of hepatic stellate cells,” *Scientific Reports*, vol. 8, no. 1, p. 2532, 2018.
- [9] S. Coulon, F. Heindryckx, A. Geerts, C. Van Steenkiste, I. Colle, and H. Van Vlierberghe, “Angiogenesis in chronic liver disease and its complications,” *Liver International: Official Journal of the International Association for the Study of the Liver*, vol. 31, no. 2, pp. 146–162, 2011.
- [10] M. McConnell and Y. Iwakiri, “Biology of portal hypertension,” *Hepatology International*, vol. 12, Supplement 1, pp. 11–23, 2018.
- [11] J. S. Lee, D. Semela, J. Iredale, and V. H. Shah, “Sinusoidal remodeling and angiogenesis: a new function for the liver-specific pericyte?,” *Hepatology (Baltimore, Md)*, vol. 45, no. 3, pp. 817–825, 2007.
- [12] K. Taura, S. De Minicis, E. Seki et al., “Hepatic stellate cells secrete angiopoietin 1 that induces angiogenesis in liver fibrosis,” *Gastroenterology*, vol. 135, no. 5, pp. 1729–1738, 2008.
- [13] H. T. Wu, Y. W. Chuang, C. P. Huang, and M. H. Chang, “Loss of angiotensin converting enzyme II (ACE2) accelerates the development of liver injury induced by thioacetamide,” *Experimental Animals*, vol. 67, no. 1, pp. 41–49, 2018.
- [14] L. Capettini, F. Montecucco, F. Mach, N. Stergiopoulos, R. Santos, and R. da Silva, “Role of renin-angiotensin system in inflammation, immunity and aging,” *Current Pharmaceutical Design*, vol. 18, no. 7, pp. 963–970, 2012.
- [15] C. H. Österreicher, K. Taura, S. De Minicis et al., “Angiotensin-converting-enzyme 2 inhibits liver fibrosis in mice,” *Hepatology (Baltimore, Md)*, vol. 50, no. 3, pp. 929–938, 2009.
- [16] R. Bataller, P. Ginès, J. M. Nicolás et al., “Angiotensin II induces contraction and proliferation of human hepatic stellate cells,” *Gastroenterology*, vol. 118, no. 6, pp. 1149–1156, 2000.
- [17] Y. Wu, Z. Li, S. Wang, A. Xiu, and C. Zhang, “Carvedilol inhibits angiotensin II-induced proliferation and contraction in hepatic stellate cells through the RhoA/Rho-kinase pathway,” *BioMed Research International*, vol. 2019, Article ID 7932046, 15 pages, 2019.
- [18] E. T. Yi, R. X. Liu, Y. Wen, and C. H. Yin, “Telmisartan attenuates hepatic fibrosis in bile duct-ligated rats,” *Acta Pharmacologica Sinica*, vol. 33, no. 12, pp. 1518–1524, 2012.
- [19] Y. M. Attia, E. F. Elalkamy, O. A. Hammam, S. S. Mahmoud, and A. S. El-Khatib, “Telmisartan, an AT1 receptor blocker and a PPAR gamma activator, alleviates liver fibrosis induced experimentally by *Schistosoma mansoni* infection,” *Parasites & Vectors*, vol. 6, no. 1, p. 199, 2013.
- [20] F. Fan, C. Tian, L. Tao et al., “Candesartan attenuates angiogenesis in hepatocellular carcinoma via downregulating AT1R/VEGF pathway,” *Biomedicine & Pharmacotherapy = Biomedicine & pharmacotherapie*, vol. 83, pp. 704–711, 2016.
- [21] R. Tamarat, J. S. Silvestre, M. Durie, and B. I. Levy, “Angiotensin II angiogenic effect in vivo involves vascular endothelial growth factor- and inflammation-related pathways,” *Laboratory Investigation; A Journal of Technical Methods and Pathology*, vol. 82, no. 6, pp. 747–756, 2002.
- [22] Q. Ding, Z. Li, B. Liu, L. Ling, X. Tian, and C. Zhang, “Propranolol prevents liver cirrhosis by inhibiting hepatic stellate cell activation mediated by the PDGFR/Akt pathway,” *Human Pathology*, vol. 76, pp. 37–46, 2018.
- [23] G. Garcia-Tsao, S. Friedman, J. Iredale, and M. Pinzani, “Now there are many (stages) where before there was one: In search of a pathophysiological classification of cirrhosis,” *Hepatology (Baltimore, Md)*, vol. 51, no. 4, pp. 1445–1449, 2010.
- [24] K. M. Mak, D. Kee, and D. W. Shin, “Alcohol-associated capillarization of sinusoids: a critique since the discovery by Schaffner and Popper in 1963,” *The Anatomical Record*, vol. 305, no. 7, pp. 1592–1610, 2022.
- [25] Y. Zheng, J. Wang, T. Zhao, L. Wang, and J. Wang, “Modulation of the VEGF/AKT/eNOS signaling pathway to regulate liver angiogenesis to explore the anti-hepatic fibrosis mechanism of curcumin,” *Journal of Ethnopharmacology*, vol. 280, article 114480, 2021.
- [26] J. Poisson, S. Lemoine, C. Boulanger et al., “Liver sinusoidal endothelial cells: physiology and role in liver diseases,” *Journal of Hepatology*, vol. 66, no. 1, pp. 212–227, 2017.
- [27] G. Czechowska, K. Celinski, A. Korolczuk et al., “The effect of the angiotensin II receptor, type 1 receptor antagonists, losartan and telmisartan, on thioacetamide-induced liver fibrosis in rats,” *Journal of Physiology and Pharmacology: An Official Journal of the Polish Physiological Society*, vol. 67, no. 4, pp. 575–586, 2016.
- [28] S. Omboni and M. Volpe, “Angiotensin receptor blockers versus angiotensin converting enzyme inhibitors for the treatment of arterial hypertension and the role of olmesartan,” *Advances in Therapy*, vol. 36, no. 2, pp. 278–297, 2019.
- [29] S. Omboni and M. Volpe, “Management of arterial hypertension with angiotensin receptor blockers: current evidence and the role of olmesartan,” *Cardiovascular Therapeutics*, vol. 36, no. 6, Article ID e12471, 2018.
- [30] T. Tsuchida and S. Friedman, “Mechanisms of hepatic stellate cell activation,” *Nature Reviews Gastroenterology & Hepatology*, vol. 14, no. 7, pp. 397–411, 2017.
- [31] S. Friedman, “Hepatic stellate cells: protean, multifunctional, and enigmatic cells of the liver,” *Physiological Reviews*, vol. 88, no. 1, pp. 125–172, 2008.
- [32] S. Cao, U. Yaqoob, A. Das et al., “Neuropilin-1 promotes cirrhosis of the rodent and human liver by enhancing PDGF/TGF- β signaling in hepatic stellate cells,” *The Journal of Clinical Investigation*, vol. 120, no. 7, pp. 2379–2394, 2010.
- [33] T. Greuter and V. Shah, “Hepatic sinusoids in liver injury, inflammation, and fibrosis: new pathophysiological insights,” *Journal of Gastroenterology*, vol. 51, no. 6, pp. 511–519, 2016.
- [34] J. S. Choi, I. S. Jeong, Y. J. Park, and S. W. Kim, “HGF and IL-10 expressing ALB::GFP reporter cells generated from iPSCs show robust anti-fibrotic property in acute fibrotic liver model,” *Stem Cell Research & Therapy*, vol. 11, no. 1, p. 332, 2020.
- [35] H. T. Nga, J. S. Moon, J. Tian et al., “Interleukin-10 attenuates liver fibrosis exacerbated by thermoneutrality,” *Frontiers in Medicine*, vol. 8, article 672658, 2021.
- [36] Y. H. Huang, M. H. Chen, Q. L. Guo, Z. X. Chen, Q. D. Chen, and X. Z. Wang, “Interleukin-10 induces senescence of activated hepatic stellate cells via STAT3-p53 pathway to attenuate liver fibrosis,” *Cellular Signalling*, vol. 66, article 109445, 2020.

- [37] Y. Iwakiri and J. Trebicka, "Portal hypertension in cirrhosis: pathophysiological mechanisms and therapy," *JHEP Reports: Innovation in Hepatology*, vol. 3, no. 4, article 100316, 2021.
- [38] G. Xie, S. S. Choi, W. K. Syn et al., "Hedgehog signalling regulates liver sinusoidal endothelial cell capillarisation," *Gut*, vol. 62, no. 2, pp. 299–309, 2013.
- [39] L. DeLeve, "Liver sinusoidal endothelial cells in hepatic fibrosis," *Hepatology (Baltimore, Md)*, vol. 61, no. 5, pp. 1740–1746, 2015.
- [40] M. Xu, X. Wang, Y. Zou, and Y. Zhong, "Key role of liver sinusoidal endothelial cells in liver fibrosis," *Bioscience Trends*, vol. 11, no. 2, pp. 163–168, 2017.
- [41] Y. Wu, Z. Li, A. Y. Xiu, D. X. Meng, S. N. Wang, and C. Q. Zhang, "Carvedilol attenuates carbon tetrachloride-induced liver fibrosis and hepatic sinusoidal capillarization in mice," *Drug Design, Development and Therapy*, vol. Volume 13, pp. 2667–2676, 2019.
- [42] A. Mallat and S. Lotersztajn, "Cellular mechanisms of tissue fibrosis. 5. Novel insights into liver fibrosis," *American Journal of Physiology Cell Physiology*, vol. 305, no. 8, pp. C789–C799, 2013.
- [43] A. Hammoutene and P. E. Rautou, "Role of liver sinusoidal endothelial cells in non-alcoholic fatty liver disease," *Journal of Hepatology*, vol. 70, no. 6, pp. 1278–1291, 2019.
- [44] M. Fernandez, "Molecular pathophysiology of portal hypertension," *Hepatology (Baltimore, Md)*, vol. 61, no. 4, pp. 1406–1415, 2015.
- [45] M. Fernández, D. Semela, J. Bruix, I. Colle, M. Pinzani, and J. Bosch, "Angiogenesis in liver disease," *Journal of Hepatology*, vol. 50, no. 3, pp. 604–620, 2009.